J|A|C|S
ARTICLES
Published on Web 11/18/2006

Disproportionation of Pyrazine in $NH^+\cdots N$ Hydrogen-Bonded Complexes: New Materials of Exceptional Dielectric Response

Andrzej Katrusiak*,† and Marek Szafrański*,‡

Contribution from the Faculty of Chemistry, Adam Mickiewicz University, Grunwaldzka 6, 60-780 Poznań, Poland, and Faculty of Physics, Adam Mickiewicz University, Umultowska 85, 61-614 Poznań, Poland

Received July 14, 2006; E-mail: katran@amu.edu.pl; masza@amu.edu.pl

Abstract: Centrosymmetric pyrazinium $NH^+\cdots N$ bonded complexes allow their dielectric properties to be analyzed separately from the bulk ferroelectric polarization observed in the noncentrosymmetric DABCO monosalts. The method of dielectric permittivity measurements has been employed for monitoring polarization fluctuations generated by proton transfers in the $NH^+\cdots N$ bonded linear polycations. The revealed dielectric response of $[C_4H_5N_2]^+BF_4^-$ and $[C_4H_5N_2]^+ClO_4^-$ cannot be reconciled with the centrosymmetric symmetry of their structures, but suggests formation of polar defects or nanoregions. Unique transformations of the pyrazine $[C_4H_5N_2]^+BF_4^-$ complex between linear $NH^+\cdots N$ hydrogen-bonded polycationic aggregates antiparallel in phase γ, perpendicular chains in phase β, and with $NH^+\cdots N$ bonds broken in phase α have been observed. The $[C_4H_5N_2]^+ClO_4^-$ and $[C_4H_5N_2]^+BF_4^-$ complexes as grown at 290 K are isostructural in orthorhombic phase γ, space group *Pbcm*, with linear polycationic chains arranged antiparallel. On heating, the tetrafluoroborate and perchlorate salts each undergoes two first-order phase transitions at similar temperatures about 340−360 K, while on cooling only one phase transition has been observed. An extremely unique sequence of two phase transitions subsequently lowering the symmetry of the $[C_4H_5N_2]^+BF_4^-$ crystal when temperature is increased has been evidenced: the orthorhombic phase γ heated above 343 K transforms into the monoclinic *C*2/*c*-symmetric phase β, in which the $NH^+\cdots N$ bonded linear chains assume perpendicular arrangement; and at about 353−357 K the anions and cations adopt a typical ionic-crystal packing without homonuclear $NH^+\cdots N$ hydrogen bonds in a still lower-symmetry monoclinic $P2_1/n$-symmetric structure. The exceptional perpendicular arrangement of the linear $NH^+\cdots N$ bonded chains in phase β constitutes a unique system where polarization of small regions can assume various orientations within a plane, depending on the H^+ sites. No phase transitions or anomalous dielectric response were observed in the $NH^+\cdots O$ bonded $[C_4H_5N_2]^+NO_3^-$ complex. The unprecedented structure−property relations of the pyrazinium complexes fully confirm the role of the $NH^+\cdots N$ bond transformations for the dielectric response of analogous DABCO ferroelectrics.

Introduction

The constant progress in the development of new smaller electronic devices depends on new materials with increasingly refined properties. The elements as basic as capacitors, or as advanced as optoelectronic transducers and actuators, require that high dielectric constant and high pyroelectric- and piezoelectric-response materials be applied. The most efficient materials, ferroelectric relaxors containing nanosized polar domains in nonpolar host matrix, are usually based on mixed perovskite structures with a considerable lead concentration. One of possible directions in the search for new Pb-free materials is to use the organic complexes where short polarized regions are formed due to the intrinsic chemical properties of the substance. The interest in dielectric properties and thermodynamic stability of pyrazine monosalts stems from the recent observations of anomalous dielectric properties,[1] ferroelectricity,[2] and relaxor-like properties[3] in dabco monosalts (dabco, or DABCO, is a commonly applied acronym of 1,4-diazabicyclo[2.2.2]octane, $C_6H_{12}N_2$). In dabco tetrafluoroborate (dabco*HBF*$_4$), perchlorate (dabco*HClO*$_4$), and perrhenate (dabco*HReO*$_4$) the dabco cations are linked into linear chains by the relatively strong homoconjugated $NH^+\cdots N$ bonds.[1,2,4] These monosalts are ferroelectric at room temperature, contrary to dabco*HBr* also comprised of linear $NH^+\cdots N$ bonded chains of the dabco cations.[5] The magnitudes of spontaneous polarization in these crystals can exceed those in any other organic and even most inorganic

† Faculty of Chemistry.
‡ Faculty of Physics.

(1) Akutagawa, T.; Takeda, S.; Hasegawa, T; Nakamura. T. *J. Am. Chem. Soc.* **2004**, *126*, 291−294.
(2) (a) Katrusiak, A.; Szafrański, M. *Phys. Rev. Lett.* **1999**, *82*, 576−579. (b) Szafrański, M.; Katrusiak, A.; McIntyre, G. *Phys. Rev. Lett.* **2002**, *89* 215507-1−215507-4.
(3) Szafrański, M.; Katrusiak, A. *J. Phys. Chem. B* **2004**, *108*, 15709−15713.
(4) Głowiak, T.; Sobczyk, L.; Grech, E. *Chem. Phys. Lett.* **1975**, *36*, 106−107.
(5) Katrusiak, A.; Ratajczak-Sitarz, M.; Grech, E. *J. Mol. Struct.* **1999**, *474*, 135−141.

ferroelectrics.[2] Moreover, the dabco monosalts exhibit a dielectric response, which can be explained in the terms of the relaxor-like behavior, and polar nanodomains embedded in the host matrix.[3] The proposed structural mechanism based on the occurrence of defects of disproportionation within supramolecular aggregates, inherent to these compounds and leading to the polar nanodomains, appears to be quite general and applicable to a wide group of substances. Indeed, the described mechanism can govern the behavior of various solid-state physical and chemical systems, where a differentiation of the constituent molecules or ions is possible, for example to charge-transfer complexes.[6] Furthermore, analogous transformations are not limited to three-dimensional crystalline structures, like H_2O ices,[7] but they have long been considered for engineered OH···O bonded supramolecules and biological systems at the molecular level[8] or for the formation of solitonic waves.[9] Like dabco, also pyrazine can exist in the molecular, monoprotonated, and diprotonated forms:

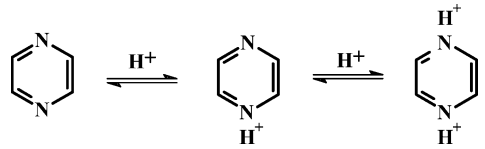

In perchlorate and tetrafluoroborate pyrazine complexes, the pyrazinium cations are NH^+···N hydrogen bonded into linear polycationic chains, analogous to those in the monosalts of dabco.[4] It was intended to check if pyrazine*HBF*$_4$, pyrazine*HClO*$_4$, and pyrazine*HNO*$_3$ crystals exhibit dielectric and thermal properties similar to those in the dabco ferroelectrics, and what is the structure of pyrazinium crystals. Unfortunately, the report on the X-ray diffraction study of pyrazine*HClO*$_4$ crystals[4] listed no structural data; they were not deposited, nor available from the authors. Thus the structure of pyrazine*HClO*$_4$ had to be redetermined. The X-ray diffraction study of pyrazine*HClO*$_4$ has been complemented by the determinations of pyrazine*HBF*$_4$ and pyrazine*HNO*$_3$ structures.

The investigated dielectric properties of the pyrazinium monosalts are intrinsically related to their chemical and thermodynamic properties. Therefore the pyrazine complexes have been studied at varied temperature. The phase transitions of dabco ferroelectrics involve conformational changes of dabco cations, proton dynamics in the NH^+···N hydrogen bonds, and ionic motions.[1,2,10] Meanwhile the planar pyrazinium rings are rigid and do not undergo any conformational transformations. Moreover, the studied pyrazinium salts are centrosymmetric at room temperature and do not exhibit ferroelectric properties. For these reasons the structures and dielectric behavior of the pyrazinium salts are of particular interest. First, it was intended to establish the role of proton dynamics in the homoconjugated NH^+···N hydrogen bonds for the possible structural transformations of the crystals and their dielectric properties. Second, the comparison of the phase transitions in the monosalts of rigid pyrazinium and conformationally flexible dabco cations could reveal the role of coupling between molecular and lattice-mode vibrations. Thus the study of the pyrazinium complexes contributes essential information for understanding structure−property relations in the dabco ferroelectrics, and in all NH···N and OH···O hydrogen-bonded substances in general.

Experimental Section

The sample crystals have been grown by evaporating the water solution of unimolar quantities of pyrazine (as bought from Aldrich, analytical grade) with appropriate acids. Pyrazine*HBF*$_4$ and pyrazine*HClO*$_4$ crystals form similar plates, as shown in Figure 1. The crystals are hygroscopic, but show no signs of decomposition after keeping them for months in dry atmosphere at 300 K. Slow sublimation of the crystals (rounding of the edges) starts at about 350-360 K, the temperature coinciding with the transition to their phase α (see below). When exposed to humid atmosphere, the crystals slowly cover with a brownish solution of the substance and its decomposition products.

The structures of pyrazine*HBF*$_4$, pyrazine*HClO*$_4$, and pyrazine*HNO*$_3$ crystals at 296 K were investigated with a KM-4 diffractometer [λ(Cu Kα) = 1.541 78 Å]. The crystal data of pyrazine*HClO*$_4$ and pyrazine*HNO*$_3$ determined at 296 K are listed in Table 1. A KM-4 CCD diffractometer [λ(Mo Kα) = 0.710 73 Å], equipped with an Oxford Cryosystem attachment, was applied for the varied-temperature studies of pyrazine*HBF*$_4$. Three crystalline phases of pyrazine*HBF*$_4$ have been studied.

The sequence of three pyrazine*HBF*$_4$ phases has been denoted with Greek-letter descriptors: the structure above 360 K has been labeled as phase α; the structure stable between 343 and 353 K and metastable down to the temperatures of liquid nitrogen has been denoted as phase β; and the structure crystallizing at room temperature and stable to 343 K has been denoted as phase γ. The transformation temperatures considerably differed from sample to sample, by several degrees, depending on their quality and thermal history. The crystal data of pyrazine*HBF*$_4$ in phase γ at varied temperatures between 296 and 341 K, of phase β in its stable temperature region at 344 K and in the metastable region at 273 K, and in phase α at 360 K have been listed in Table 2. The structures of pyrazine*HClO*$_4$ and pyrazine*HNO*$_3$ crystals, as well as of three pyrazine*HBF*$_4$ phases, were solved straightforwardly by direct methods[12] and refined by least-squares on reflections intensities.[13] The hydrogen atoms in the room-temperature phases were located from the difference Fourier maps and refined with isotropic thermal parameters. The carbon hydrogens in the structures of phases α and β of pyrazine*HBF*$_4$ were re-determined from the molecular geometry after each cycle of refinement and included in the structure-factor calculations. The acidic proton in phase α structure was located from the difference Fourier map and refined. In the *C*2/*c*-symmetric β phase the pyrazinium cation is located on an inversion center, and consequently the proton is disordered with equal occupancies at the two nitrogen atoms. It was attempted to lower the space group symmetry of phase β to check the possibility of ordered proton in a pseudosymmetric structure. For example, the protons with fractional site-occupancy factors (SOF's) in the *C*2-symmetric β-phase structures of pyrazine*HBF*$_4$, both at 344 K and in the metastable region at 273 K, were assigned to two nitrogen atoms at the idealized locations. The occupation of these sites was constrained to refine as one free variable SOF for the site at N(1), and (1 − SOF) for the site at N(4). The values of SOF refined to 0.61(17) for the structure at 344 K and to 0.29(18) for the metastable structure at 273 K. Thus these locations of the protons in the lower-symmetry β phase structures were not

(6) Horiouchi, S; Kumai, R; Okimoto, Y; Tokura Y. *Phys. Rev. B* **1999**, *59*, 11267−11275.
(7) Nylund, E. S.; Tsironis, G. P. *Phys. Rev. Lett.* **1991**, *66*, 1886−1889.
(8) (a) Nagle, J. F.; Mille, M.; Morovitz, H. J. *J. Chem. Phys.* **1980**, *72*, 3959−3971. (b) Etter, M. C.; Urbańczyk-Lipkowska, Z.; Jahn, D. A.; Frye, J. S. *J. Am. Chem. Soc.* **1986**, *108*, 5871−5869.
(9) Davidov, A.S. *Solitony v molekularnyh systemah* [*Solitons in molecular systems*, in Russian]; Naukova Dumka: Kiev, Russia, 1984.
(10) <ovd>Zoga]-O. J.; Galewski, Z.; Grech, E.; Malarski, Z. *Mol. Phys.* **1985**, *56*, 673−681.
(11) Katrusiak, A. *J. Mol. Graphics Modell.* **2001**, *19*, 363−367.
(12) Sheldrick, G. *SHELXS-97 Program for solving crystal structures*; University of Goettingen: Goettingen, Germany, 1997.
(13) Sheldrick, G. *SHELXL-97 Program for crystal structure determination*; University of Goettingen: Goettingen, Germany, 1997.

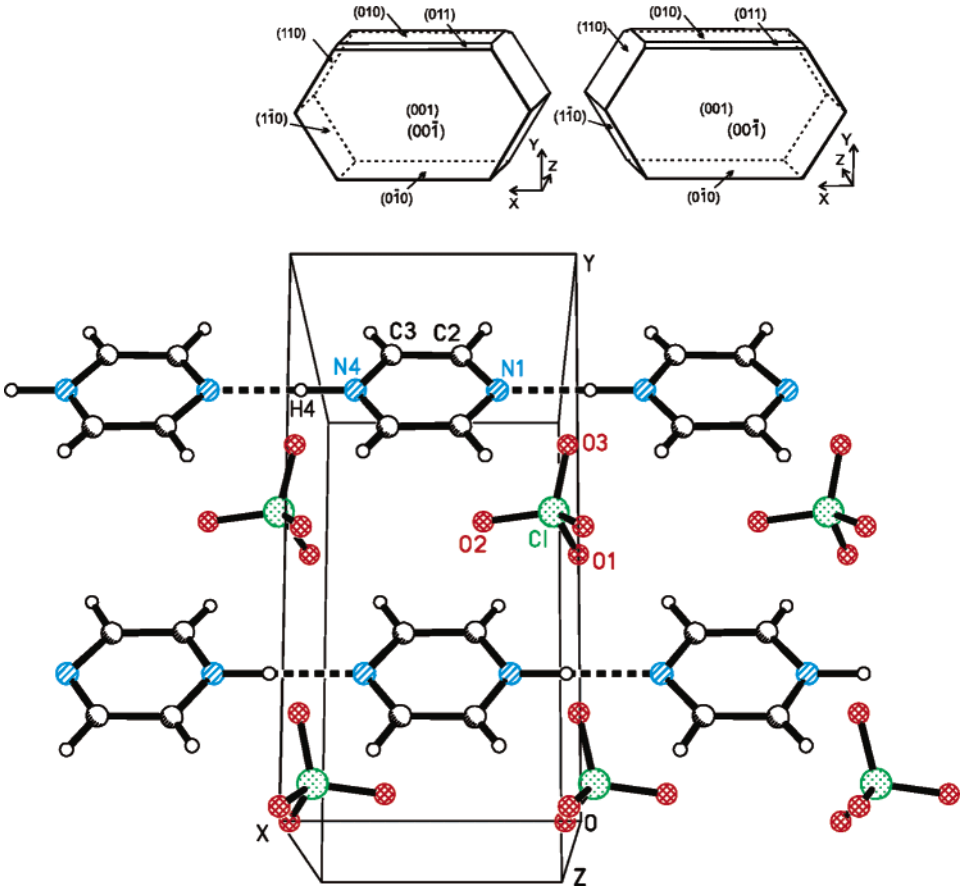

Figure 1. PyrazineHBF_4 crystal grown from aqueous solution at 290 K. Usually plates with the largest (001) faces and small or even nonexisting (011) faces are formed (the case shown in this stereographic scheme); however occasionally faces (011) can grow even larger than the (001) faces—probably due to the crystal location in the crystallization vessel. Below: an autostereogram[11] of the structure of pyrazine$HClO_4$ at 296 K, isostructural with pyrazineHBF_4 phase γ. The hydrogen bonds are shown as thick dashed lines and the H-atoms as small circles; only the atoms in one symmetry-independent part of the unit cell have been labeled in this drawing.

Table 1. Selected Crystal Data for Pyrazine$HClO_4$ and PyrazineHNO_3 at 296 K

	pyrazine$HClO_4$	pyrazineHNO_3
empirical formula	$[C_4H_5N_2]^+ \cdot ClO_4^-$	$[C_4H_5N_2]^+ \cdot NO_3^-$
formula wt	180.55	143.11
cryst syst	orthorhombic	monoclinic
space group	*Pbcm*	$P2_1/c$
unit cell dimens		
a (Å)	5.5535(6)	6.9950(10)
b (Å)	11.0663(14)	8.722(2)
c (Å)	11.3243(8)	10.182(2)
β (deg)	90	105.18(2)
V (Å^3)	695.95(13)	599.5(2)
Z	4	4
calcd dens (g/cm^3)	1.723	1.586
F(000)	368	296
goodness-of-fit on F^2	1.117	1.032
final R1/wR2 indices	0.0566/0.1435	0.0433/0.1311

conclusive; moreover, the Hamilton's *R*-factor tests allowed rejection of the hypothesis that the structure symmetry is lower than *C*2/*c*. In light of these results the proton is indeed disordered between its N(1) and N(4) sites. The detailed information about the diffraction studies and the structural results have been deposited with the Cambridge Crystallographic Database Center as supplementary publications number CCDC 280226 for pyrazine$HClO_4$, CCDC 289227 for pyrazineHNO_3; CCDC 289228, CCDCC 606622, CCDC 606621, and CCDC 606620 for pyrazineHBF_4 phase γ at 296, 303, 338 and 341 K; CCDC 606617 and CCDC 606618 for pyrazineHBF_4 phase β in the stable temperature region at 344 K and in the metastable region at 273 K; and CCDC 606619 for phase α at 360 K, respectively. The atomic coordinates, temperature parameters, and molecular dimensions have been listed in the Supporting Information.

Calorimetric measurements were performed by differential thermal analysis (DTA) between 120 and 390 K. The polycrystalline samples were prepared by grinding the single-crystals into fine powder. In the heating and cooling runs the temperature was changed at the rate of 3 K/min.

Complex dielectric permittivity was measured with a HP 4192A impedance analyzer in the frequency range between 10 kHz and 10 MHz. The samples for dielectric studies were prepared in the form of plate capacitors. The silver-paste electrodes were deposited on the (001) faces of pyrazineHBF_4 and pyrazine$HClO_4$ crystals in phase γ, which were the best naturally developed faces of the crystals grown from aqueous solution (Figure 1). It should be noted that the morphology—structure relation established for phase γ is irrelevant to phases β and α, where the H-bonding pattern is transformed.

Results and Discussion

Calorimetric and dielectric measurements on pyrazineHBF_4 and pyrazine$HClO_4$ showed that these two substances, obtained at room temperature in phase γ, when heated transform to phase β, and at still higher temperature to phase α, and that phase β is metastable when cooled to room temperature for days or hours, depending on the history of the sample. In the first DTA heating runs of both the pyrazineHBF_4 and pyrazine$HClO_4$ powder samples, there are two overlapping thermal anomalies corresponding to two successive first-order phase transitions. As can be seen from the DTA plots shown in Figure 2, the

Table 2. Selected Crystal Data for Phases γ, β, and α of PyrazineHBF_4 at Varied Temperature[a]

	phase γ				phase β		phase α
temp (K)	296 K	303 K	338 K	341 K	344 K	273 K	360 K
cryst syst	orthorhombic	orthorhombic	orthorhombic	orthorhombic	monoclinic	monoclinic	monoclinic
space group	*Pbcm*	*Pbcm*	*Pbcm*	*Pbcm*	*C*2/*c*	*C*2/*c*	$P2_1/n$
Unit-cell dimens							
a (Å)	5.5452(7)	5.5438(18)	5.5555(13)	5.5588(9)	7.823(2)	7.802(2)	8.1160(16)
b (Å)	10.8198(13)	10.813(4)	10.845(3)	10.872(2)	7.838(2)	7.828(2)	8.5140(17)
c (Å)	11.1006(9)	11.120(3)	11.191(4)	11.189(3)	11.208(3)	11.075(3)	10.311(2)
β (deg)	90	90	90	90	97.44(3)	97.83(2)	108.04(3)
V (Å^3)	666.01(16)	666.6(4)	674.3(3)	676.2(3)	681.5(4)	670.1(3)	677.5(2)
Z	4	4	4	4	4	4	4
dens (g/ cm^3)	1.675	1.673	1.654	1.649	1.637	1.664	1.646
goodness-of-fit on F^2	1.001	1.118	1.128	1.204	1.001	1.117	1.037
final R1/wR2 indices	0.044/0.130	0.051/0.121	0.061/0.139	0.081/0.167	0.0443/0.1300	0.0566/0.1435	0.058/0.141

[a] The data of phase β in its stable region at 344 K and about 70 K below its $T_{\gamma\beta}$ transition temperature in the metastable region at 273 K have been presented.

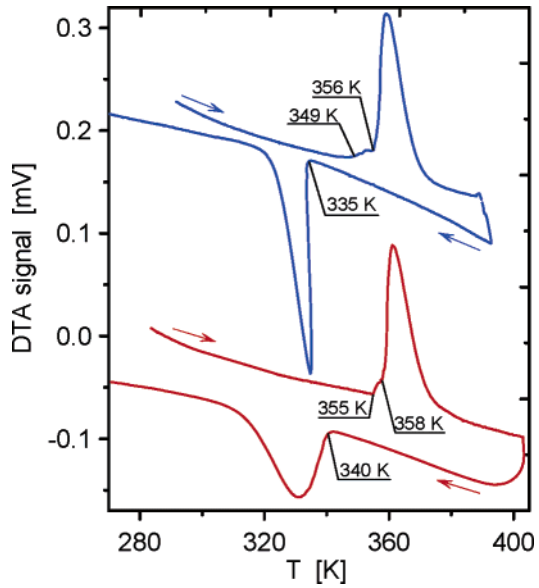

Figure 2. DTA signals for pyrazineHBF_4 (blue) and pyrazine$HClO_4$ (red) measured for the samples heated and cooled, as indicated by arrows. The plot for pyrazineHBF_4 was shifted upward to avoid overlapping.

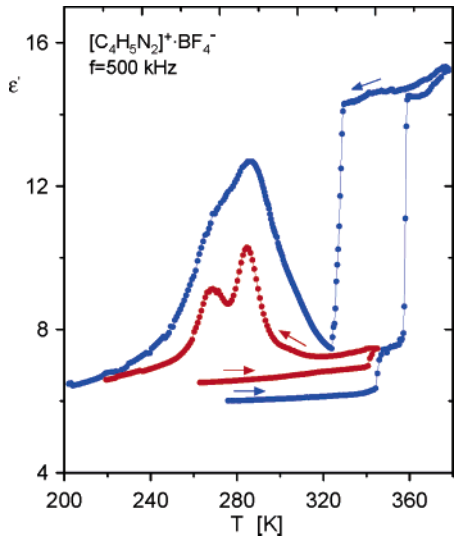

Figure 3. Real part of dielectric permittivity of the pyrazineHBF_4 crystals heated and subsequently cooled through the temperature range including both γ-to-β and β-to-α phase transitions (blue points) and through the temperature range ended below the transition to the high-temperature phase α (red points). Two different samples were used for both temperature cycles; the arrows indicate the sequence of measurements.

large anomalous DTA signals are preceded by the small ones. For pyrazineHBF_4 the onsets of these anomalies occur at 349 and 356 K, respectively, while only one thermal anomaly with the onset at 335 K appears on cooling the sample. A similar sequence of phase transitions was revealed for pyrazine$HClO_4$: two transitions at 355 and 358 K in the first heating cycle and only one at 340 K on cooling the sample. It is remarkable that in the second and successive heating cycles both crystals underwent only a single transformation corresponding to the large anomaly seen in Figure 2. It testifies that the intermediate phase β is metastable.

The conclusions based on the calorimetric measurements are supported by the temperature dependence of dielectric response of the crystal, presented in Figure 3. In the first heating cycle the pyrazineHBF_4 crystal clearly undergoes two first-order phase transitions manifested by two steplike anomalies in the temperature dependence of the real part of electric permittivity $\epsilon'(T)$. The increase in ϵ' is especially high at the transition to the high-temperature phase α. This anomalous dielectric increment is most probably related to the triggering of the ionic dynamics, which can significantly contribute to the electric permittivity through the local dipolar fluctuations. It is apparent that, on cooling, the reverse transition to the intermediate phase β occurs with a large temperature hysteresis and the crystal remains in this phase even at low temperatures, much below the room temperature. This is suggested by the magnitude of ϵ', which does not match that of phase γ. Moreover, on cooling the sample, a new singularity in $\epsilon'(T)$ occurred around 275 K. This double-peak anomaly can be attributed to the specific properties of the crystal phase β, as testified by the results shown in Figure 3. The virgin crystal heated to the temperature range of phase β and then immediately cooled down clearly exhibited the unusual dielectric response, but no anomaly, which could be associated with the reverse transition to phase γ, could be detected. The dielectric anomalies were observed both on cooling and heating the sample that was previously transformed to the intermediate phase β. It should be pointed out that some differences in the magnitudes of ϵ' measured for virgin crystals were most probably due to the distribution of lattice defects, specific for the individual samples.

Detailed observations of the phase-transition temperatures have been monitored by dielectric-permittivity measurements for various samples of pyrazineHBF_4, for example freshly crystallized or crystallized 6 months earlier, or of different history of thermal treatment. It occurred that the temperatures

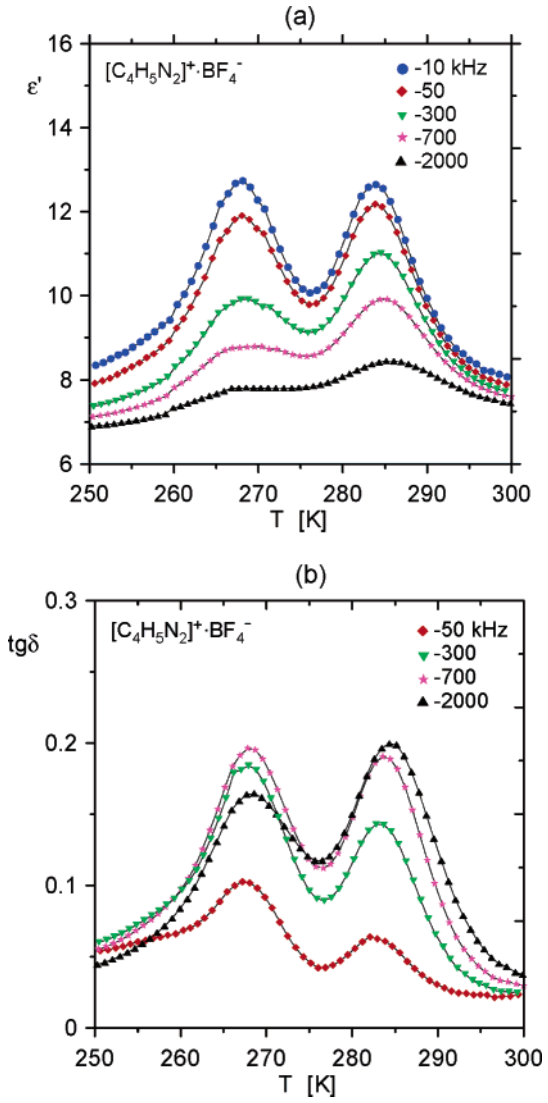

Figure 4. Frequency and temperature dependencies of (a) the real part of dielectric permittivity and (b) the tangent of dielectric losses measured for pyrazineHBF_4 in metastable phase β on heating the sample. Before transforming to the β phase, the single-crystal sample was oriented with the [001] direction along the applied field.

of transformations varied from 343 to 349 K for the γ-to-β transformation and between 353 and 357 K for the β-to-α transition. The virgin samples transformed at higher temperatures. Irrespective of the temperature value, all these transitions proceeded in a sharp manner and exhibited no diffused character. Such differences of the transition temperatures can be accounted for by defects in conjunction with the presence of metastable regions formed in these hydrogen-bonded structures.

The maxima in the temperature dependencies of ϵ' and the tangent of dielectric losses (tan δ) show a profound frequency dispersion, as seen in Figure 4. This type of dielectric behavior can be interpreted as an indication of the presence of an additional contribution to the dielectric response of the crystal. The origin of this striking new phenomenon can be related to the specific features of linear $NH^+\cdots N$ hydrogen-bonded aggregates in the crystal structures of pyrazineHBF_4 and pyrazine$HClO_4$, similar to those observed in the analogous crystals of the dabco*HA* monosalts (*HA* stands for the mineral acid).[3] To analyze the origin of the dielectric response of pyrazineHBF_4 in phase β, the Cole−Cole formalism was applied. As shown in Figure 5a the Cole−Cole plots form semiarcs with their centers located much below the ϵ' axis, indicating that the dielectric relaxation has a strongly polydispersive character. In such a case the complex electric permittivity was modeled with the following Cole−Cole function:[14]

$$\epsilon = \epsilon_\infty + \frac{\epsilon_s - \epsilon_\infty}{1 + (i\tau\omega)^{1-k}} \qquad (1)$$

where ϵ_s and ϵ_∞ are the low-frequency and high-frequency limiting values of the real part of electric permittivity, τ is the most probable relaxation time, k is a measure of the distribution of relaxation times, and ω is the angular frequency. For assessing the possible contribution of electric conductivity, a related term has been included into the equation used for describing the experimental data:

$$\epsilon = \epsilon_\infty + \frac{\epsilon_s - \epsilon_\infty}{1 + (i\tau\omega)^{1-k}} + \frac{i\sigma}{\omega\epsilon_0} \qquad (2)$$

where σ is the electric conductivity in [nS m^{-1}] and ϵ_0 is the vacuum permittivity. The solid lines in Figure 5a represent the best fits of eq 2 to the experimental points at several temperatures. The fitting procedure showed that the electric conductivity, ranging between 0.2 and 7.8 nS m^{-1}, is relatively small and does not contribute significantly to the dielectric response. The electric conductivity considerably increases above about 356 K, when an onset of sublimation has been observed, and the pyrazineHBF_4 crystals transform into the α phase, in the structure of which the ionic motions are intensified.

The exponent k values indicate a broad distribution of the relaxation rates. As can be inferred from the temperature dependence of k, plotted in the inset in Figure 5a, the distribution function of the relaxation rates progressively broadens with decreasing temperature. Such a behavior is characteristic of dipolar glass formation.[15] The Arrhenius plot of the relaxation time and the temperature dependence of the dielectric relaxation strength $\Delta\epsilon = \epsilon_s - \epsilon_\infty$ are shown in Figure 5b. Apparently, the dielectric data in the entire experimental range cannot be rationalized, neither by a single Arrhenius law[16] nor by the single Vogel−Fulcher−Tammann[17] law. On the other hand, the fittings to the data points in the limited temperature regions result in extremely low unrealistic activation energies. The temperature dependence of τ testifies that the dielectric relaxation in pyrazineHBF_4 phase β has a complicated nature, and several relaxators contribute to the total dielectric response of the crystal in the studied temperature and frequency ranges.

(14) Cole K. S.; Cole, R. H. *J. Chem. Phys.* **1941,** *9*, 341−351.
(15) Loidl, A.; Böhmer, R. In *Disorder effects on relaxational processes*; Richert, R., Blumen, A., Eds.; Springer-Verlag: Berlin, Heidelberg, 1994; pp 659−696.
(16) Glasstone, S.; Laider, K. J.; Eyring, H. *The theory of rate processes*, McGraw-Hill: New York, 1941.
(17) Vogel, H. *Phys. Z.* **1921**, *22*, 645−646. Fulcher, G. S. *J. Am. Ceram. Soc.* **1925,** *8*, 339−355.

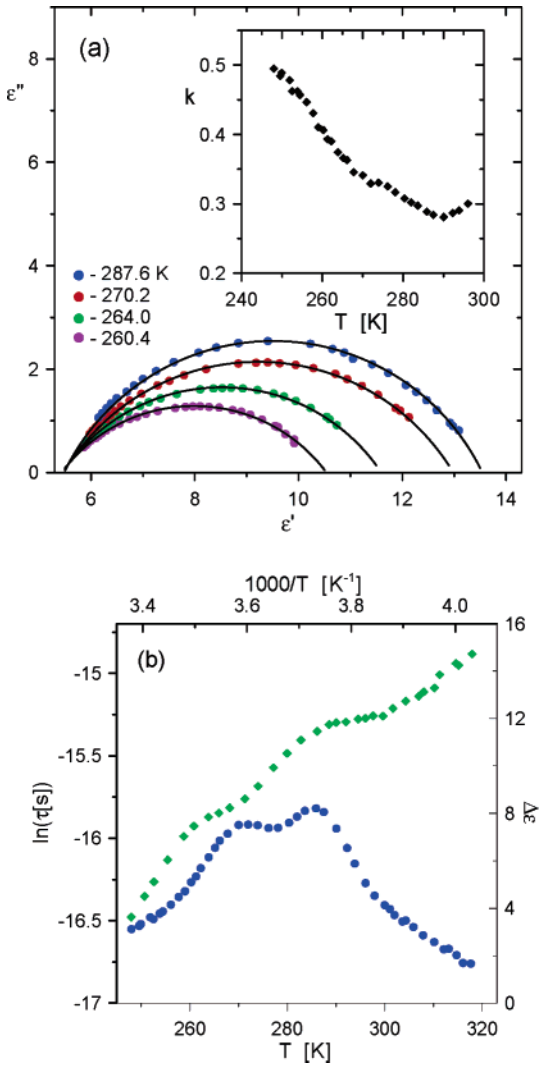

Figure 5. (a) Cole−Cole plots for pyrazineHBF_4 in the temperature range of the dielectric anomalies observed in the metastable phase β. The solid lines represent the best fits of eq 2 to the experimental points; the temperature dependence of the k exponent is shown in the inset. (b) Arrhenius plot of the relaxation time (green points) and temperature dependence of the dielectric strength (blue points).

Pyrazine$HClO_4$ and PyrazineHBF_4 Phase γ. The pyrazine$HClO_4$ and pyrazineHBF_4 crystals are isostructural at 296 K. The unit-cell dimensions are similar within 0.25 Å (see Tables 1 and 2), with the unit-cell volume of pyrazine$HClO_4$ by nearly 30 Å^3 larger than that of pyrazineHBF_4, i.e., 7.5 Å^3 per one formula unit (one ionic pair). The crystals are built of cations hydrogen bonded into linear antiparallel chains along [100], as shown in Figure 1. The protons and the N atoms of the cationic chains are located on the 2-fold axes parallel to [100], while the anions are located on the mirror planes perpendicular to [001]. The polarization of the chains is alternated along [010], while the chain neighbors along [001] have the same polarization. One link of the chains, consisting of one cation, is commensurate with one unit cell dimension along [100], which is also characteristic of the dabco monosalts. The dimensions of the hydrogen bonds in pyrazine$HClO_4$ and pyrazineHBF_4 in phase γ, listed in Table 3, are similar to those in dabco analogues, too.

Structure of PyrazineHBF_4 in Phase β. The crystal structure of pyrazineHBF_4 in the β phase, shown in Figure 6, is unique in this respect that the chains of NH$^+$···N bonded pyrazinium anions run in two approximately perpendicular directions [1$\bar{1}$0] and [$\bar{1}$10]. The exact inclination angle of these directions projected on the (001) plane is 89.81(2)° at 273 K and 89.89(3)° at 344 K—thus it is very weakly temperature-dependent, approaching 90° when temperature rises. The N····N distance in the hydrogen bond becomes slightly, by 0.013 Å, longer at 344 K (Table 4). The transannular N···N distance would be shortened by the ring rotations, but it is hardly affected by the temperature increase [2.716(3) Å at 273 K and 2.714(4) Å at 344 K], which confirms that the pyrazinium cations are orientationally ordered. Due to the center-of-inversion site symmetry of the cations, the protons in phase β are disordered with equal occupancies of 0.5 between two nitrogen atoms in the NH$^+$···N bonds [protons are ordered at N(4) in phase γ and at N(1) in phase α].

The role of the proton disordering for the phase transition of pyrazineHBF_4 and the stability of the β phase is still not clear, although now it is evident that proton disordering can be a common phenomenon related to the low disproportionation energy of the molecular, monocationic, and dicationic forms of pyrazine. A similar behavior was observed in dabco*HBr* and dabcoHBF_4 crystals. It thus appears that pyrazine exhibits similar properties. This disproportionation is essential for the relaxor-like behavior observed in the dabcoHBF_4 crystals. The distance between the sites of the disordered protons is 1.10 and 1.13 Å at 273 and 344 K, respectively.

The β phase is also exceptional because of its large temperature hysteresis—it can exist for days even 100 K below its stability region, and due to this property the structural determination at 273 K could be performed. The unique perpendicular arrangement of the NH$^+$···N bonded chains has significant consequences for the dielectric properties, discussed below.

Structure of PyrazineHBF_4 in Phase α. At about 357 K pyrazineHBF_4 transforms to $P2_1/n$-symmetric phase α (Table 2). Its structure, shown in Figure 7, when compared to the lower-temperature phases of pyrazineHBF_4, illustrates a unique phase transition changing the physical and chemical nature of the compound. At the β-to-α phase transition pyrazineHBF_4 changes its chemical character from the homonuclear NH$^+$···N bonded complex in phase β (Figure 6) to the chemical complex in phase α where the NH$^+$···N bonds between pyrazinium anions are broken, and only very weak heteronuclear NH$^+$···F bonds link pyrazinium and BF_4^- ions. These very weak NH$^+$···F bonds are systematically formed and broken following the quick rotations of the orientationally disordered anions. The shortest contacts of the proton and partially occupied fluorine atoms sites have been listed in Table 5.

The van der Waals radius of the fluorine atom is between 1.33 and 1.58 Å and of N of about 1.5 Å,[18] so the H···F distances in the structure of phase α can be considered as weak hydrogen bonds. The ions are evenly surrounded by counter ions (Table 6). In the α phase at 360 K, the distance from the boron atom to the protonated N(4) atom is by 0.139(13) Å closer than to deprotonated N(1). However the closest distance of the anion center is to carbon atom C(2), which confirms the transformation of the hydrogen-bonded complex to a typical ionic structure governed by electrostatic forces.

(18) Batsanov, S. S. *Inorg. Mater.* **2001**, *37*, 871. Batsanov, S. S. *Strukturnaia khimia−Fakty i zavisimosti* [*Stuctural chemistry−Book of facts*, in Russian]; Dialog MGU: Moscow, 2000.

Table 3. Dimensions of Hydrogen Bonds at 296 K in Phase γ of Pyrazine*HClO₄* and Pyrazine*HBF₄*, and in Pyrazine*HNO₃*

crystal	D–H···A	D···A (Å)	D-H (Å)	H···A (Å)	D–H···A (deg)
pyrazine*HClO₄* (β)	N(1)-H(1)···N(4[a])	2.828(6)	1.05(10)	1.78(10)	180
pyrazine*HBF₄* (γ)	N(1)−H(1)···N(4[a])	2.838(3)	1.01(4)	1.82(4)	180
pyrazine*HNO₃*	N(1)−H(1)···O(1)	2.733(3)	0.95(4)	1.79(4)	168.0(8)

[a] Symmetry code: $x - 1, y, z$.

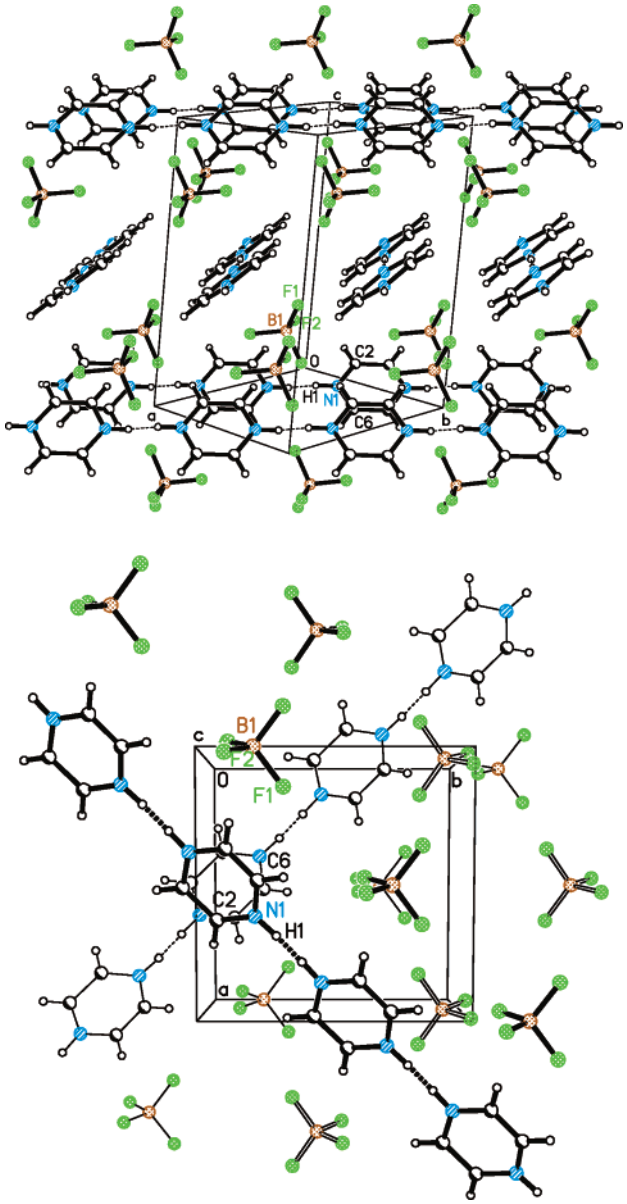

Figure 6. Pyrazine*HBF₄* structure in phase β at 273 K: (a) autostereographic projection approximately down [110] and (b) two NH⁺···N bonded chains of pyrazinium cations in the pyrazine*HBF₄* structure in phase β at 273 K, viewed down the [001] direction. The upper chain (closer to the viewer) is drawn with thick lines, and the lower chain is drawn with thin lines. Similarly, the uppermost layer of BF_4^- anions has been drawn with thick lines, this in the middle with double open lines, and this at the bottom with thin single lines. Partially occupied sites of the acidic proton at N(1) and N(4) atoms of the pyrazinium cation have been shown, and the hydrogen bonds are indicated by the thin dashed lines.

In the NH⁺···N bonded phases of pyrazine*HBF₄*, the boron atom is located at about 3.4 Å from the nitrogen atoms and at about 3.8 Å to the carbon atoms, while the closest distances between N and F are longer than 3.0 Å.

Table 4. NH⁺···N Hydrogen-Bond Dimensions in the β Phase of Pyrazine*HBF₄* at 273 and 344 K[a]

N–H···N	N···N (Å)	N-H (Å)	H···N (Å)	N–H···N (deg)
273 K				
N(1)−H(1)···N(1[b])	2.811(3)	0.86	1.952	176.7
344 K				
N(1)−H(1)···N(1[b])	2.824(5)	0.86	1.965	177.2

[a] The dimensions involve the partially occupied proton site at N(1) with the occupancy factor of 0.5. [b] Symmetry code: $0.5 - x, 1.5 - y, 1.0 - z$.

Structure of Pyrazine*HNO₃*. The crystals of pyrazine*HNO₃* are built of NH⁺···O bonded ionic pairs. The hydrogen-bonded planar cation and planar anion are approximately coplanar and approximately parallel to the crystallographic plane ($10\bar{1}$). The H-bonded ionic pairs are arranged into planar corrugated sheets, shown in Figure 8 (and in Figure S2 in Supporting Information). The dimensions of the hydrogen bond are given in Table 3. The shortest of other contacts are O(1)···H(2[i]) of 2.307 Å ([i]symmetry code: $1 - x, 0.5 + y, 0.5 - z$), O(2)···H(6) of 2.358 Å, O(2)···H(5[ii]) of 2.474 Å ([ii]symmetry code: $1 - x, y - 0.5, 0.5 - z$), and N(4) ···H(6[i]) of 2.610 Å.

No phase transition has been detected for pyrazine*HNO₃*, which confirms that the proton behavior in the homonuclear hydrogen bonds plays a crucial role in the transformations of pyrazine*HClO₄* and pyrazine*HBF₄*. In the NH⁺···O hydrogen bond in pyrazine*HNO₃*, the H-dynamics—even if present in some form—cannot trigger proton motions concerted with the lattice-mode vibrations, nor switch the structure between domains of reverse polarization. The absence of the anomalous dielectric properties and phase transitions in pyrazine*HNO₃* corroborates the structural explanations of the properties of the pyrazine*HBF₄* crystals presented below. It was shown most recently that dabco*HBr* undergoes a structural transformation between the complex with homonuclear NH⁺···N bonds to the complex with heteronuclear NH⁺···Br⁻ bonds.[19] That reversible transformation is triggered by modest pressure of 400 MPa. It is thus possible that analogous complexes can exist around defects in the crystal structure at ambient conditions, which would considerably contribute to the macroscopic properties of these hydrogen-bonded complexes.

Structure−Property Relation in Pyrazine*HClO₄* and Pyrazine*HBF₄*. The structures of pyrazine*HClO₄* and pyrazine*HBF₄* are strongly anisotropic: not only direction [100] is very different from directions [010] and [001], but also directions [010] and [001] are different between themselves (see projection down the [100] direction in the Supporting Information). In this respect the pyrazine monosalts in phase γ are considerably different from the dabco analogues. The different type of interactions along [010] and [001] is for example reflected in the unit-cell thermal expansion of the crystals. When the crystals are heated, the difference between parameters *b* and *c* increases (the difference between parameters perpendicular to the H-

(19) Budzianowski, A.; Katrusiak, A. *J. Phys. Chem. B* **2006**, *110*, 9756−9758.

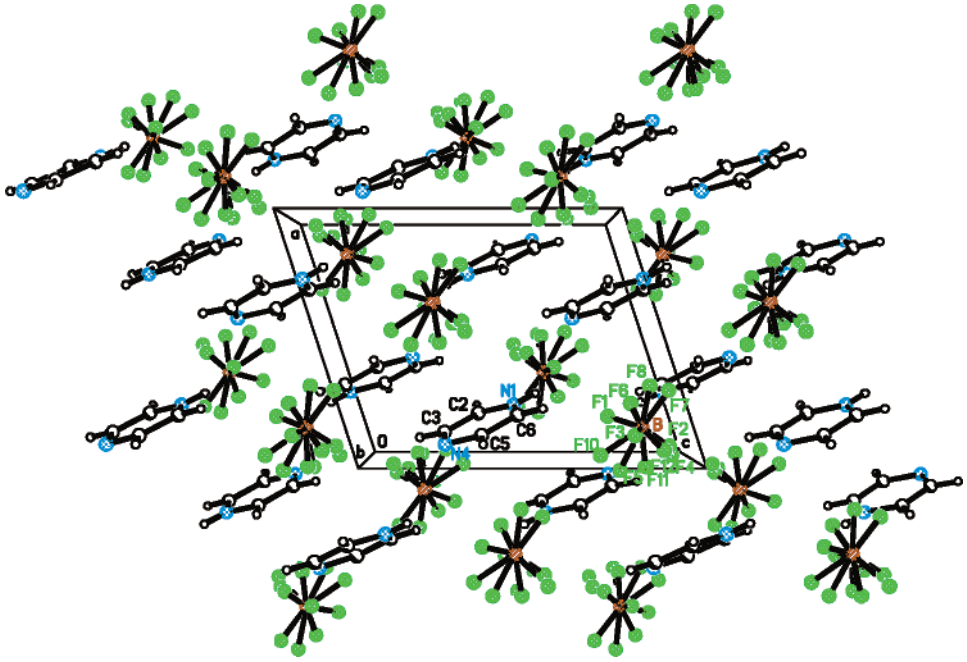

Figure 7. Autostereographic projection of pyrazineHBF_4 in phase α at 360 K. The partially occupied sites of fluorine atoms in the orientationally disordered BF_4^- anions have been shown.

Table 5. Shortest Contacts of the Proton at N(1) and Partially Occupied Fluorine-Atom Sites of the Orientationally Disordered BF_4^- Anion in the α-Phase of PyrazineHBF_4[a]

D-H···A	D···A (Å)	D-H (Å)	H···A (Å)	D–H···A (deg)
N(1)−H(1)···F(4[b])	2.894(11)	0.86	2.159	164.3
N(1)−H(1)···F(5)	2.880(12)	0.86	2.366	103.5
N(1)−H(1)···F(6[b])	2.794(12)	0.86	2.137	149.0
N(4)···F(3[c])	3.222(12)			
N(4)···F(4[d])	3.221(12)			

[a] The two shortest contacts of the N(4) atom have also been listed for comparison. [b] Symmetry code: $0.5 - x, y - 0.5, 1.5 - z$. [c] Symmetry code: $x - 0.5, 1.5 - y, z - 0.5$. [d] Symmetry code: $-x, 2.0 - y, 1.0 - z$.

Table 6. Shortest Distance of Each N and C Atom of the Cation to the Central B-Atom of the BF_4 Anions

cation-atom···B(anion)	distance (Å)	symmetry code of B-atom
N(1)···B	3.849(9)	$0.5 - x, y - 0.5, 1.5 - z$
N(4)···B	3.988(9)	$x - 0.5, 1.5 - y, z - 0.5$
C(2)···B	3.797(10)	$0.5 - x, y - 0.5, 1.5 - z$
C(3)···B	3.916(11)	$-x, 1.0 - y, 1.0 - z$
C(5)···B	3.915(10)	$x - 0.5, 1.5 - y, z - 0.5$
C(6)···B	3.900(11)	x, y, z

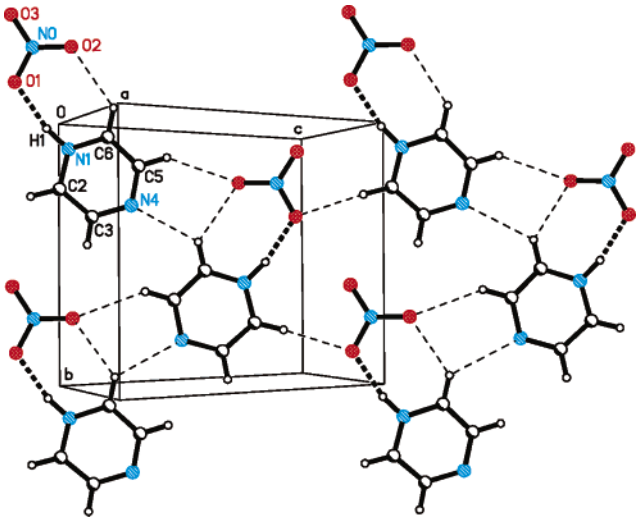

Figure 8. Autostereogram of the crystal structure of pyrazineHNO_3 at 296 K viewed perpendicular to one sheet along crystal plane $(10\bar{1})$ (the view along the sheets is shown in Figure S2 in Supporting Information). The hydrogen bonds are shown as thick dashed lines and the shortest interionic contacts as thin dashed lines.

bonded dabco chains decreased in heated crystals). Apparently, the planar shape of the aromatic rings in pyrazine$HClO_4$ and pyrazineHBF_4 contributes to this anisotropy and to different behavior of the salts of pyrazine than of their dabco analogues. The dabco crystals transform to the tetragonal phases, with directions [x] and [y] equivalent, the H-bonded polycationic chains parallel, and triggered rotations of the cations around the N···N axis. Phase γ of pyrazine$HClO_4$ and pyrazineHBF_4 transform into a monoclinic phase β, where the cations are ordered, but the directions of the H-bonded chains become nearly perpendicular. In the highest-temperature crystalline phase α of pyrazine$HClO_4$ and pyrazineHBF_4 the anions become orientationally disordered (like in the dabco H-bonded complexes), but the cations remain ordered, which can be attributed to their planar shape.

The sequence of symmetry changes accompanying the phase transitions in pyrazineHBF_4 is unusual in this respect that the symmetry decreases for the higher-temperature phases. The space groups of phases γ, β, and α are *Pbcm* (symmetry class *mmm*), *C*2/*c* (2/*m*), and $P2_1/n$ (2/*m*), respectively. To our knowledge, such a symmetry reduction in a sequence of two transitions to higher-temperature phases has not been accounted for. The reverse group−subgroup relation exists between phases γ and α (when space group *Pbcm* transforms to $P2_1/n$, the following symmetry elements disappear: 2-fold axis parallel to [x], glide plane b perpendicular to [x], screw axis 2_1 parallel to [z], and mirror plane m perpendicular to [z]); and between phases β and α (when space group *C*2/*c* is reduced to space group $P2_1/n$, 2-fold axis parallel to [y] and glide plane c perpendicular to [y] disappear). Thus ferroelastic domains are

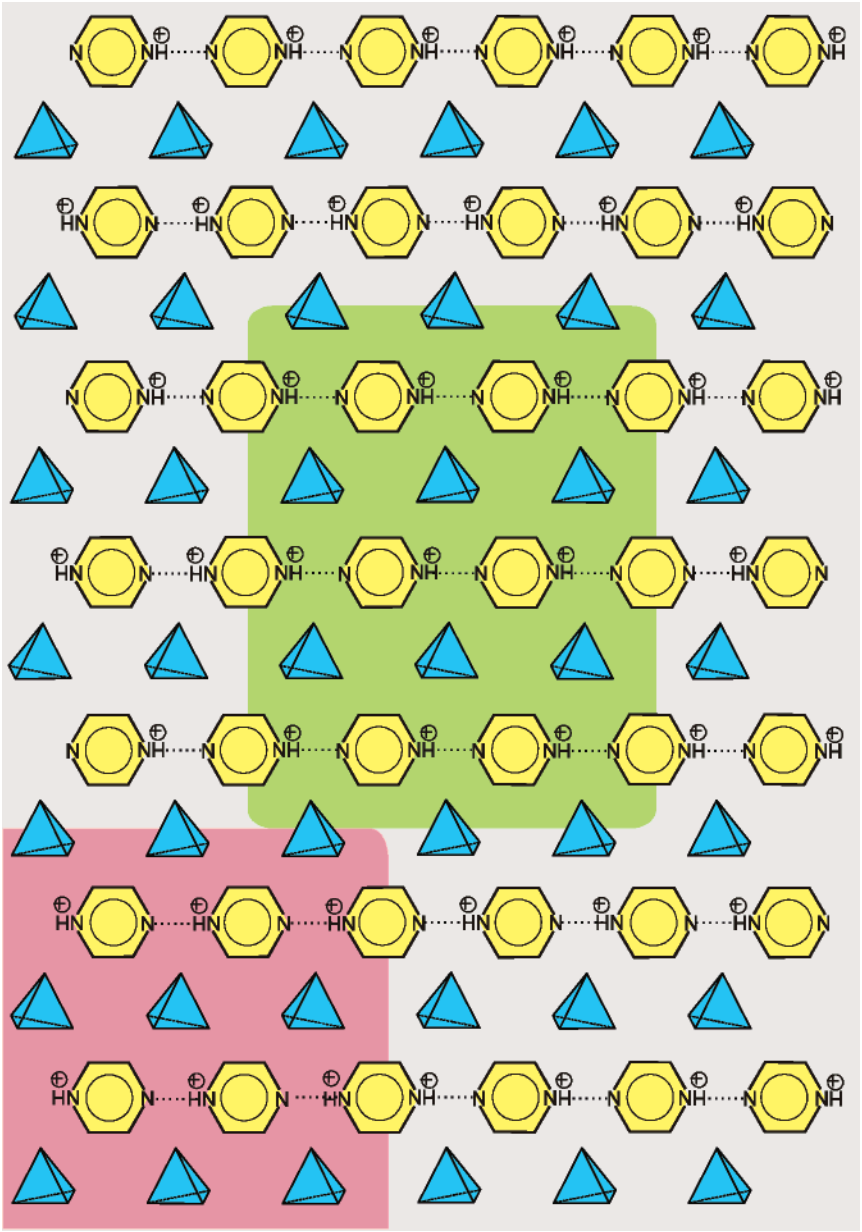

Figure 9. Schematic representation of a fragment the hydrogen-bonded pyrazine*HBF₄* (or pyrazine*HClO₄*) structure: in the array of ideally antiparallel $NH^+\cdots N$ hydrogen-bonded chains (gray), a polar nanodomain (marked green) results from protons transferred in the sequence of three $NH^+\cdots N$ hydrogen bonds in the interval between the dication (left) and neutral molecule (right) of the fourth chain. In another oppositely polarized nanoregion generated due to H^+-transfers in the bottom chain, indicated in red, the dication is at the right wall of the region. The BF_4^- anions are represented as blue tetrahedra. A perfect fragment of the crystal, with the chains composed of monocations only, has been shown at the top of this drawing, and in a separate Figure S4 in the Supporting Information.

formed in the heated sample transforming between phases γ and β, and this domain structure persists in the metastable phase β and also in the stable phase α. The domain structure can be held responsible for the observed anomalous dielectric response around 275 K. The transformation between the parallel and perpendicular H-bonding networks and domains shuttering of the crystal structure are bound to lead to the formation of polarized regions in the networks of hydrogen bonds, which contribute considerably to the dielectric response of the crystal.

These structural features appear to indicate that the proton behavior in the $NH^+\cdots N$ hydrogen bonds plays a crucial role for the phase transitions of the pyrazine*HBF₄* and pyrazine*HClO₄* crystals. It was shown that the $NH^+\cdots N$ bonds polarizability is strongly environment-dependent[20] and that the proton sites are coupled to the orientations and positions of the counter ions in the ionic crystals.[21] Like dabco, also pyrazine can exist in the molecular, monoprotonated, and diprotonated forms. The transitions between α, β, and γ phases of pyrazine*HBF₄* confirm, that disproportionation energy between these forms is very low. In particular, the disordered proton location in the β phase of pyrazine*HBF₄*, both for the stable temperature region of the β phase and in its metastable region extending by over 100 K below, may be connected with dynamic disordering of the protons, but also to the effect of very high density of dispro-

(20) (a) Rabold, A.; Bauer, R.; Zundel, G. *J. Phys. Chem.* **1995**, *99*, 1889−1895.; (b) Brzeziński, B.; Zundel, G. *J. Chem. Soc., Faraday Trans. 2* **1983**, *79*, 1249−1257.
(21) Katrusiak, A. *J. Mol. Struct.* **1999**, *474*, 125−133.

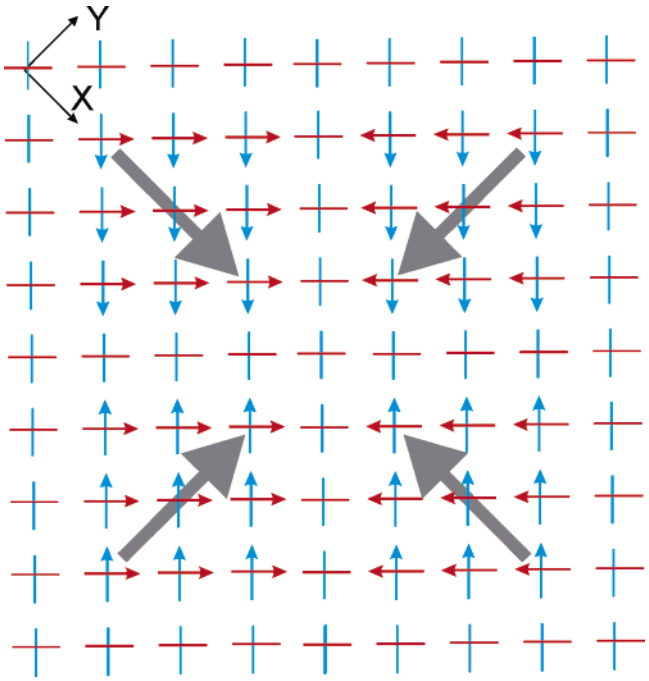

Figure 10. Examples of four possible configurations of short-range polar regions in the β-phase of pyrazineHBF_4 (or pyrazine$HClO_4$). The pyrazinium monocations have been schematically represented as red arrows (upper layer) and blue arrows (lower layer), while the dashes (without arrowheads) represent neutral molecules and dications. The BF_4^- anions have been neglected for clarity. Ideal regions with layers of three polarized chains, each with three monocations, have been presented, and the resulting polarization indicated with a large gray arrows along directions [x], [y], [$-y$], and [$-x$].

portionation defects. Such defects are likely to be generated during the phase transitions. Hence, the dielectric properties of the crystals depend on their history. The observed dielectric behavior confirms that the pyrazine monosalts with homonuclear hydrogen bonds are prone to such structural defects. Each proton transfer in the $NH^+\cdots N$ hydrogen bond has its immediate consequences for the crystal structure: (i) a proton transfer between two monocations creates a small domain with its two domain walls along the chain—a molecular and dicationic pyrazine; (ii) a proton transfer from the monocation to the molecule extends or reduces the domain at its negative-polarized end; (iii) a proton transfer from the dication to the monocation extends or reduces the domain at its positive-polarized end; (iv) a proton transfer from the dication to the molecule annihilates the domain.

Any molecular or dicationic pyrazine constitutes a domain wall reversing the polarization of the adjacent H-bonded chain fragments, as illustrated in Figure 9. The defects of this kind are particularly prone to occur at the structural phase transitions. Thus in principle the H-transfers can generate structural defects contributing to the dielectric response of the pyrazineHBF_4 and pyrazine$HClO_4$ crystals.

Due to the perpendicular arrangement of the $NH^+\cdots N$ hydrogen-bonded chains in phase β, the short-range polar regions can assume practically any polarization in the (001) plane, depending on the number of dipoles and their directions. Examples of the configurations of the regions acquiring polarizations along [x], [y], [$-x$], and [$-y$] are shown in Figure 10.

Conclusions

The group of known natural and synthesized substances with a prominent role of hydrogen bonds has considerably grown during the past half-century, but for a long time ferroelectric properties have been associated exclusively with the strong OH···O hydrogen bonds.[22] Only recently ferroelectric properties were evidenced in the NH···N bonded systems[2] and in the all-organic cocrystals with strong OH···N bonds.[23−25] The structure and properties of the pyrazineHBF_4 and pyrazine$HClO_4$ crystals provide new evidence of the role of $NH^+\cdots N$ hydrogen bonds for the phase transitions and dielectric behavior of the materials. The properties of the pyrazineHBF_4 and pyrazine$HClO_4$ crystals cannot be reconciled with their centrosymmetric symmetry, but they can originate from short-range polar regions in these structures. It has been demonstrated that the conformational properties of the recently studied dabco $NH^+\cdots N$ bonded complexes are not necessary conditions for their relaxor-like properties. There are still questions, which should be clarified. For example, if the shape of tetrahedral anions is important for the transformations and properties of the dabco and pyrazine $NH^+\cdots N$ bonded complexes with mineral acids. Our results indicate that the essential element of the observed behavior is the system of homonuclear hydrogen bonds with a weak correlation between the protons and low disproportionation energy between molecules, monocations, and dications.

The sequence of phase transitions in pyrazineHBF_4 is exceptional in several respects. The most remarkable physical aspect is the reverse group−subgroup symmetry relation between phases, where symmetry elements disappearing with the rising temperature. Another unusual feature is the transformation of the chemical character of this substance, which in the γ phase is a typical $NH^+\cdots N$ bonded complex of amino base with a mineral acid. In the β phase the homonuclear $NH^+\cdots N$ bonds rearrange, so the H-bonded chains run at nearly perpendicular directions, and the protons become disordered in the hydrogen bonds. Finally, in the α phase the $NH^+\cdots N$ bonds are broken and pyrazineHBF_4 acquires a typical ionic-crystal structure (with very weak $NH^+\cdots F$ bonds) and the protons are ordered, while the anions become orientationally disordered. It is plausible that the extremely exceptional reverse symmetry changes between the phases of pyrazineHBF_4 are a consequence of the changing chemical character of this substance. The γ phase is strongly anisotropic, with the $NH^+\cdots N$ bonded chains running along [x]. In the β phase the $NH^+\cdots N$ bonded chains are approximately perpendicular in the structure; thus in this respect the β phase is more isotropic than the γ phase of the crystal. The α phase is least anisotropic, as the $NH^+\cdots N$ aggregates do not exist in its structure. Thus the sequence of γ-to-β-to-α phase transitions consecutively changes the dimensionality of the system—with the increasing temperature it becomes less anisotropic and more isotropic. Such increasing isotropic features of the crystal are very often consistent with increased symmetry, for example from triclinic, to monoclinic, orthorhombic, tetragonal, and cubic systems. However most of

(22) Lines, M. E.; Glass, A. *Principles and applications of ferroelectrics and related materials*; Oxford University Press: New York, 1977.
(23) Horiuchi, S.; Ishii, F.; Kumai, R.; Okimoto, Y.; Tachibana, H.; Nagaosa, N.; Tokura, Y.; *Nat. Mater.* **2005**, *4*, 163−166.
(24) Horiuchi, S.; Kumai, R.; Tokura, Y. *J. Am. Chem. Soc.* **2005**, *127*, 5010−5011.
(25) Asaji, T.; Gotoh, K.; Watanabe, J. *J. Mol. Struct.* **2006**, *791*, 89−92.

known phase transitions do not change the chemical character of the materials. The example of pyrazine*HBF_4* suggests that the increasing isotropic structure of a system is the primary trend in transformations of substances with increasing temperature. More systematic studies of the properties of crystals are still required for better documenting this conclusion.

Acknowledgment. This study was supported by the Polish Committee of Scientific Research, Grant No 3T09A01511.

Supporting Information Available: Tables of crystal structures data, atomic coordinates, bond lengths and angles, and anisotropic thermal parameters, projections of crystal structures for pyrazineHBF_4 and pyrazineHNO_3, and a scheme of a perfect pyrazineHBF_4 structure. This material is available free of charge via the Internet at http://pubs.acs.org.

JA0650192